Published in final edited form as:
Neurobiol Dis. 2012 March ; 45(3): 1101–1110. doi:10.1016/j.nbd.2011.12.028.

Metabotropic Glutamate Receptor-dependent Long-term Depression is Impaired Due to Elevated ERK Signaling in the ΔRG Mouse Model of Tuberous Sclerosis Complex

Itzamarie Chévere-Torres[1], **Hanoch Kaphzan**[1], **Aditi Bhattacharya**[1], **Areum Kang**[1], **Jordan M. Maki**[1], **Michael J. Gambello**[2], **Jack L. Arbiser**[3], **Emanuela Santini**[1], and **Eric Klann**[1,†]

[1]Center for Neural Science, New York University, New York, NY 10003

[2]Division of Medical Genetics, Department of Pediatrics, University of Texas Health Science Center at Houston, Houston, TX 77030

[3]Department of Dermatology, Emory University School of Medicine, Atlanta, GA 30322

Abstract

Tuberous sclerosis complex (TSC) and fragile X syndrome (FXS) are caused by mutations in negative regulators of translation. FXS model mice exhibit enhanced metabotropic glutamate receptor-dependent long-term depression (mGluR-LTD). Therefore, we hypothesized that a mouse model of TSC, ΔRG transgenic mice, also would exhibit enhanced mGluR-LTD. We measured the impact of TSC2-GAP mutations on the mTORC1 and ERK signaling pathways and protein synthesis-dependent hippocampal synaptic plasticity in ΔRG transgenic mice. These mice express a dominant/negative TSC2 that binds to TSC1, but has a deletion and substitution mutation in its GAP-domain, resulting in inactivation of the complex. Consistent with previous studies of several other lines of TSC model mice, we observed elevated S6 phosphorylation in the brains of ΔRG mice, suggesting upregulated translation. Surprisingly, mGluR-LTD was not enhanced, but rather was impaired in the ΔRG transgenic mice, indicating that TSC and FXS have divergent synaptic plasticity phenotypes. Similar to patients with TSC, the ΔRG transgenic mice exhibit elevated ERK signaling. Moreover, the mGluR-LTD impairment displayed by the ΔRG transgenic mice was rescued with the MEK-ERK inhibitor U0126. Our results suggest that the mGluR-LTD impairment observed in ΔRG mice involves aberrant TSC1/2-ERK signaling.

Keywords

tuberous sclerosis complex; TSC2; TSC1; mTORC1; ERK; fragile x syndrome; mGluR-LTD; NMDAR-LTD

Introduction

Tuberous sclerosis complex (TSC) is an autosomal dominant disorder that can cause hamartomas, benign and malignant neoplasms, seizures, mental impairment and autism,

†To whom correspondence should be addressed: Eric Klann, Ph.D., Center for Neural Science, New York University, 4 Washington Place, Room 809, New York, NY 10003, eklann@cns.nyu.edu, phone: (212) 992-9769, fax: (212) 995-4011.

(DiMario, 2004). At the molecular level, TSC is caused by either the loss or malfunction of either hamartin (TSC1) or tuberin (TSC2), which interact in a heterodimer known as the TSC1/TSC2 complex, to negatively regulate mammalian target of rapamycin complex 1 (mTORC1) (Cheadle et al., 2000). mTORC1 functions as a molecular gatekeeper for cap-dependent translation initiation in neurons. Activation of the phosphoinositide 3-kinase (PI3K)/Akt and extracellular signal-regulated kinase (ERK) signaling pathways results in the phosphorylation of TSC2 and inhibition of the GTPase-activating protein (GAP) activity of TSC2, which leads to increased levels of Rheb-GTP. This type of signaling activates the mTOR complex 1 (mTORC1) and subsequent phosphorylation ribosomal S6 kinase 1 (S6K1) and eukaryote initiation factor 4E-binding protein (4E-BP), key translation initiation regulators (Cai et al., 2006; Jozwiak, 2006; Jozwiak et al., 2005; Orlova and Crino, 2010; Yang et al., 2006).

It has been estimated that sporadic cases of TSC range from 60 to 70% of the cases reported, and that *TSC1* mutations are significantly underrepresented compared to *TSC2* (Jones et al., 1997). *TSC2* gene mutations are more frequent and result in a more severe phenotype in TSC patients (i.e. seizures and learning disability), with the exception of reported cases of patients with no mutation identified, as well as one *TSC2* mutation that causes a more mild phenotype (Camposano et al., 2009; Dabora et al., 2001; Jansen et al., 2006; Kwiatkowski, 2003). In addition, the *TSC2* gene is more prone than the *TSC1* gene to large deletions, rearrangements, and missense mutations. Of particular interest is the finding that missense mutations are clustered within *TSC2* exons 34–38, which encode for either Rap1GAP or GAP3 (Maheshwar et al., 1997). The TSC2-GAP domain is an essential structural domain for the hydrolysis of GTP-bound Rheb to its inactive GDP-bound form (Tee et al., 2003).

Studies have shown that either loss or malfunction of TSC1 and TSC2 usually results in activation of S6K1 and enhanced ribosomal protein S6 phosphorylation, resulting in defective regulation of cell size and proliferation (Krymskaya, 2003; Uhlmann et al., 2004). Moreover, studies in hippocampal pyramidal neurons have shown that the TSC pathway regulates soma size, the density and size of dendritic spines, and the properties of excitatory synapses, particularly AMPA receptor-mediated currents (Tavazoie et al., 2005). Additional studies have shown that loss of TSC1 function in the brain leads to neocortical hyperexcitability associated with increased glutamate-mediated excitation in both human tissue and mouse brain (Wang et al., 2007). Finally, TSC2 heterozygous knockout mice were shown to exhibit elevated hippocampal mTORC1 signaling, which led to abnormal long-term potentiation (LTP) and deficits in hippocampus-dependent memory (Ehninger et al., 2008).

The ΔRG transgenic mouse has been developed, carrying a deletion in TSC2 of amino acid residues 1617–1655 and a substitution of amino acid residues 1679–1742, which interferes with both the GAP domain and rabaptin-5 binding motif of TSC2, respectively (Govindarajan et al., 2005; Pasumarthi et al., 2000). As a result, this dominant/negative TSC2 protein is not able to hydrolyze GTP-bound small G-proteins, such as Rap1 and Rheb (Govindarajan et al., 2005; Pasumarthi et al., 2000; Zhang et al., 2003). Previous studies have shown that ΔRG transgenic mice have increased expression of the dominant/negative TSC2 driven by the cytomegalovirus (CMV) promoter and develop skin and brain abnormalities consistent with those observed in TSC patients (Bhatia et al., 2009; Govindarajan et al., 2005; Sambucetti et al., 1989). In addition, behavioral studies on ΔRG mice have revealed increased anxiety levels and mild deficits in hippocampus-dependent learning and memory, consistent with TSC-related neuropsychiatric symptoms (Ehninger and Silva, 2010; Chévere-Torres et al., 2012).

Fragile X syndrome (FXS) is caused by loss of function mutations in the RNA-binding protein, fragile X mental retardation protein (FMRP), whose normal function is to suppress translation (Ronesi and Huber, 2008). Consistent with this notion, mouse models of FXS display increased protein synthesis, enhanced mTORC1 signaling, and exaggerated metabotropic glutamate receptor-dependent long-term depression (mGluR-LTD) (Hou et al., 2006; Huber et al., 2002; Osterweil et al., 2010; Sharma et al., 2010). Based on evidence that both TSC1/2 and FMRP proteins act as negative regulators of protein synthesis and mTORC1 signaling, and the evidence that patients with TSC and FXS can both display autism spectrum disorder, we hypothesized that the mutations in TSC2-GAP domain in ΔRG mice would result in similar synaptic plasticity alterations and mTORC1 dysregulation as observed in other mouse models of TSC and FXS model mice. Herein we describe experiments with the ΔRG transgenic mice that were conducted to determine whether they exhibit hippocampal synaptic plasticity phenotypes consistent with other mouse models of TSC and FXS.

Materials and Methods

Animals

ΔRG Transgenic Mice—Generation of ΔRG mice has been described previously (Govindarajan et al., 2005). Mouse genotyping was performed by PCR using transgene- and wild-type-specific primer sets.

Tsc1 Floxed Mice—Mice with floxed *Tsc1* (mixed genetic background composed of C57Bl/6J, 129/SvJae, BALB/cJ) were generated as described previously (Kwiatkowski et al., 2002). For the generation of experimental mice, we crossed heterozygous floxed *Tsc1* ($TSC1^{+/-}$) male mice and heterozygous floxed *Tsc1* ($TSC1^{+/-}$)-α*CaMKII-Cre* females. Mice were genotyped using *Cre*-specific primers and primers that identify floxed alleles of the *Tsc1* locus. The wild-type mice used in this study were $TSC1^{+/+}$-αCaMKII-Cre and the experimental conditional heterozygous mice used in this study were $TSC1^{+/cko}$-αCaMKII-Cre (referred to as $TSC1^{+/-}$ cKO) mice.

Tsc2 Floxed Mice—Mice with floxed *Tsc2* (mixed genetic background composed of C57Bl/6J, 129/SvJae) were generated as described previously (Hernandez et al., 2007). For the generation of experimental mice, we crossed heterozygous floxed *Tsc2* ($TSC2^{+/-}$) male mice and heterozygous floxed *Tsc2* ($TSC2^{+/-}$)-α*CaMKII-Cre* females. Mice were genotyped using *Cre*-specific primers and primers that identify floxed alleles of the *Tsc2* locus. The wild-type mice used in this study were $TSC2^{++}$-αCaMKII-Cre and the experimental conditional homozygous mice used in this study were $TSC2^{cko/cko}$-αCaMKII-Cre (referred to as $TSC2^{-/-}$ cKO) mice.

For all experiments, male age-matched littermates were used. For biochemical experiments, 4–12 week-old mice were used, for LTP experiments 8–12 week-old mice were used, and 4–6 week-old mice were used for mGluR-LTD experiments. Mice were kept on a 12 h on-off light/dark cycle. Food and water were available at all times. All procedures were approved by the New York University Animal Care and Use Committee and followed the NIH Guidelines for the use of animals in research.

Western Blot Analysis

Protein extracts were prepared by homogenizing hippocampal tissue in ice-cold hypotonic lysis buffer (HLB) containing phosphatase and protease inhibitor mixtures. Homogenates (20 μg) were resolved via 4–12% SDS-PAGE and transferred to polyvinylidene difluoride (PVDF) membranes. Immunobloting was performed using standard techniques. Rabbit

polyclonal antibodies were used to detect phospho-S6 (S235/236), phospho-S6 (S240/244), total S6, phospho-S6K1 (T389), and total S6K1 at a 1:1000 dilution (Cell Signaling Technologies, Beverly, MA). 1:1000 rabbit anti-phospho-S6K1 (T389, Millipore Corp., Billerica, MA). A monoclonal antibody was used to detect TSC1 levels at a 1:1000 dilution (Cell Signaling, Beverly, MA) in 5% BSA blocking solution. TSC2 levels were detected using a monoclonal antibody (CellSignaling, Beverly, MA) at a 1:1000 dilution in 5% BSA blocking solution. The dilution used for phospho-4E-BP (T37/46) and total 4E-BP antibodies was 1:500 (Cell Signaling Technologies, Beverly, MA) in 5% BSA/I-Block. Phospho-ERK (T202/Y404) and total ERK antibodies were diluted at 1:2000. β–actin and α-tubulin antibodies (Sigma-Aldrich, St. Louis, MO) were diluted 1:10,000 in 5% milk/T-TBS. Anti-rabbit and anti-mouse HRP-tagged antibodies (Promega, Madison, WI) were diluted 1:5000 in 0.2% I-Block (Tropix, Foster City, CA) and 1:10,000 in 5%Milk/T-TBS, respectively. Blots were developed using enhanced chemiluminescence detection (GE Healthcare, Fairfield, CT).

Immunohistochemistry and Histology

Saggital sections (40 μm thick) were blocked with 1% BSA and incubated overnight at 4°C with TSC2 rabbit monoclonal antibody (1:200; Epitomics, Burlingame, CA) in 1% BSA. Sections were washed with PBS and incubated with secondary antibody for 30 min. Sections then were incubated with ABC reagent (Pierce, Rockford, IL) and immunostaining was visualized using the VIP substrate kit for peroxidase (Vector Laboratories, Burlingame, CA). Brains from a different set of mice were used for histological studies. Saggital sections (40 μm thick) were mounted onto subbed slides. Nissl staining was performed according to standard procedures. Sections from immunohistochemistry and Nissl staining were viewed and photographed using a BX51 Olympus microscope (Olympus, UK) and Neurolucida 7 software (MBF Bioscience, Willinston, VT).

Electrophysiology

Brains from age-matched littermate mice were removed and transverse hippocampal slices (400 μm) were prepared. Hippocampal slices were placed in cold-cutting solution (in mM: 110 sucrose, 60 NaCl, 3 KCl, 1.25 NaH_2PO_4, 28 $NaHCO_3$, 5 D-glucose, 0.6 Ascorbic Acid, 0.5 $CaCl_2$, and 7 $MgCl_2$, gassed with 95% O_2/5% CO_2). The slices were incubated with a 50:50 cutting/artificial CSF (ACSF) solution (in mM: 125 NaCl, 2.5 KCl, 1.25 NaH_2PO_4, 25 $NaHCO_3$, 25 D-glucose, 2 $CaCl_2$, and 1$MgCl_2$) for 15 min, followed by equilibration for 1 hr in a humid, oxygenated interface chamber continuously perfused with 32°C ACSF at a rate of 2ml/min. Field excitatory postsynaptic potentials (fEPSPs) were evoked by stimulation of the Schaeffer collateral pathway and recorded in stratum radiatum of area CA1 using a glass recording pipette (1–4 MΩ). Stimulus intensity was adjusted to elicit a fEPSP that was 50% of the maximum response in each slice. Baseline measurements were taken for 30 min prior to delivery of a single train of high-frequency stimulation (HFS; 100 Hz for 1 sec) to induce early phase LTP (E-LTP), prior to delivery of four, spaced trains of HFS (100 Hz for 1 sec, 5 min intertrain interval) to induce late phase LTP (L-LTP), for 20 min prior to treatment with DHPG (50μM, 10min; Ascent, Princeton, NJ) to induce mGluR-LTD, or for 20 min prior to deliver 900 pulses of low-frequency stimulation (LFS; 1Hz, 15 min) to induce N-methyl D-aspartate NMDA-LTD. When indicated, ACSF was supplemented with U0126 (1mM, Promega, Madison, WI). For LTD rescue experiments, baseline measurements were taken for 30 min prior to application of DHPG (50μM, 10min) in the presence of U0126 (1μM). Afterward, fEPSPs were evoked and recorded in the stratum radiatum of area CA1 in the presence of the inhibitor for 1 hour.

Statistical Analysis

Graph Pad Prism data analysis software (San Diego, CA) was used for graph production and statistical analysis was used to assess the data. Student's *t*-tests and two-way ANOVAs were used for biochemical and electrophysiological data analysis, respectively. Data represent mean±SEM, with $p<0.05$ used as significance criteria.

Results

ΔRG mice exhibit normal hippocampal LTP but impaired mGluR-dependent LTD

First, we confirmed the presence of the ΔRG transgene (Fig. 1A) by PCR techniques, detecting a band of 280bp (Fig. 1B). We determined whether the loss of TSC2-GAP function in ΔRG mice resulted in aberrant hippocampal morphological changes. Nissl staining of sections from ΔRG mice indicated they have normal gross hippocampal morphology (Fig. 1C). To determine whether TSC2 levels were increased, we examined hippocampal tissue from ΔRG mice and their wild-type littermates with immunocytochemistry and observed increased TSC2 levels in ΔRG mice compared to their wild-type controls (Fig. 1D), consistent with previous studies (Bhatia et al., 2009).

Because mice with mutations in negative modulators of translation exhibit altered synaptic function (Richter and Klann, 2009), we examined several forms of hippocampal synaptic plasticity in slices from ΔRG mice. Analysis of synaptic output in response to increasing stimulatory input indicated that the basal synaptic transmission was normal in hippocampal area CA1 of the ΔRG mice (Fig. 2A). Fiber volley amplitude measured with increasing stimulation also was unaltered in ΔRG mice (Fig. 2B). We next examined paired-pulse facilitation (PPF), a short-lasting form of presynaptic plasticity evoked by temporally linked stimuli, and found that PPF was unaltered in ΔRG mice using both short and long interpulse intervals (Fig. 2C). We proceeded to determine whether the ΔRG mice exhibited altered long-term potentiation (LTP). We used a single train of high-frequency stimulation (HFS) to induce early phase LTP (E-LTP) and four, spaced trains of HFS to induce protein synthesis-dependent late phase LTP (L-LTP) in hippocampal slices from wild-type and ΔRG mice. We observed that both E-LTP and L-LTP in ΔRG mice were indistinguishable from that in their wild-type littermates (Fig. 3A and 3B). Thus, basal synaptic transmission, PPF, E-LTP, and L-LTP are unaltered in ΔRG mice.

Previous studies have shown that a mouse model of fragile X syndrome (FXS) exhibits enhanced hippocampal mGluR-LTD due to improper regulation of translation and its uncoupling from mGluR signaling (Ronesi and Huber, 2008; Sharma et al., 2010; Osterweil et al., 2010). In addition, clinical studies have shown increased immunoreactivity for group I mGluRs (mGluR1/5) and phosphorylated ribosomal protein S6 within cortical tubers and subependymal giant-cell tumors of TSC specimens (Boer et al., 2008), suggesting upregulation of mGluR-mTORC1 signaling similar to that observed in FXS model mice (Sharma et al., 2010). Therefore, we hypothesized that hippocampal mGluR-dependent LTD would be enhanced in the ΔRG mice. Hippocampal slices from ΔRG mice and their wild-type littermates were treated with DHPG (50 μM, 10 min), a selective agonist of group I mGluRs, which resulted in a pronounced initial depression of synaptic transmission in both ΔRG and wild-type mice (Fig. 3C). This depression rapidly returned to near baseline levels in ΔRG mice after drug washout, whereas in wild-type mice it was followed by a robust long-lasting depression (Fig. 3C). This finding indicates that mutations affecting the TSC2-GAP domain result in an impairment of mGluR-LTD in the hippocampus. To determine the receptor specificity of the LTD deficit in ΔRG mice, low-frequency stimulation (LFS) was utilized to induce N-methyl D-aspartate receptor-dependent LTD (NMDAR-LTD) in hippocampal slices from ΔRG mice and their wild-type littermates. We observed that

NMDAR-LTD in ΔRG mice was identical to that of their wild-type littermates (Fig. 3D). These findings indicate that the impaired LTD is specific to altered mGluR-dependent signaling in the ΔRG mice.

We next tested whether mGluR-LTD also was impaired in mice with a heterozygous conditional deletion of *Tsc1* ($TSC1^{+/-}$ cKO) and homozygous conditional deletion of *Tsc2* ($TSC2^{-/-}$ cKO) in postnatal forebrain neurons under the control of the αCaMKII promoter (α*CamKII-Cre*) (Supplementary Fig. 1). We found that both $TSC1^{+/-}$ cKO and $TSC2^{-/-}$ cKO mice exhibited significant impairments in mGluR-LTD compared to their wild-type controls (Fig. 4A and 4B). Further analysis and comparison of the average fEPSP slopes from ΔRG, $TSC1^{+/-}$ cKO and $TSC2^{-/-}$ cKO hippocampal slices during the time period of 20 to 50 min after DHPG application revealed that all three TSC mouse models have a similar level of LTD impairment (Fig. 4C). These findings indicate that disruption of the TSC1/2 complex either by conditional deletion of *Tsc*1/2 genes or by mutations affecting the TSC2-GAP domain results in deficient mGluR-LTD expression in the hippocampus.

Hippocampal mTORC1 signaling in ΔRG mice

The impairment in mGluR-LTD led us to examine mTORC1 signaling in hippocampal homogenates from the ΔRG mice. Western blot analysis indicated that although phosphorylation of serine 235/236 on ribosomal protein S6 was elevated in the ΔRG mice, phosphorylation of serine 240/244, a rapamycin-sensitive/mTORC1-dependent site, was unaffected (Fig. 5A). Moreover, phosphorylation of eukaryotic initiation factor 4E-binding protein (4E-BP) and p70 S6 kinase 1 (S6K1), direct substrates of mTORC1, were not altered in the ΔRG mice (Fig. 5B). Because phosphorylation of serine 235/236 on S6 can be regulated by both mTORC1 and ERK signaling (Pende et al., 2004; Roux et al., 2004), we examined ERK1/2 phosphorylation in the hippocampus of ΔRG mice. We observed that the ΔRG mice exhibited a robust increase in ERK1/2 phosphorylation compared to their wild-type littermates (Fig. 5C). These findings suggest that the impaired mGluR-LTD observed in ΔRG mice is not a direct consequence of elevated mTORC1 signaling as initially postulated, but could be related to aberrant TSC1/2-ERK signaling.

We also examined ERK1/2 phosphorylation in the hippocampus of $TSC1^{+/-}$ cKO and $TSC2^{-/-}$ cKO mice to determine whether enhanced ERK signaling also is a feature of TSC1/2 deletion in the brain. We found that ERK phosphorylation was not affected in the hippocampus of either $TSC1^{+/-}$ cKO or $TSC2^{-/-}$ cKO mice (Fig. 6A and 6B). These data suggest that a distinct molecular mechanism may be responsible for the deficit observed in mGluR-LTD in $TSC1^{+/-}$ cKO and $TSC2^{-/-}$ cKO mice, while the mGluR-LTD impairment and aberrant ERK1/2 activation observed in ΔRG mice is because of TSC2-GAP mutations in ΔRG mice.

Inhibition of MEK-ERK signaling rescues mGluR dependent-LTD in ΔRG mice

Our findings of enhanced ERK phosphorylation led us to examine the contribution of MEK-ERK signaling to the impaired mGluR-LTD exhibited by the ΔRG mice. In wild-type mice, mGluR-LTD requires activation of both mTORC1 and MEK-ERK signaling (Banko et al., 2006; Gallagher et al., 2004; Hou and Klann, 2004; Sharma et al., 2010). We utilized the MEK inhibitor U0126 (Favata et al., 1998) and performed dose/response experiments in hippocampal slices from wild-type mice in an attempt to find an effective dose at which levels of ERK phosphorylation were reduced but not completely blocked and did not compromise the integrity of mGluR-LTD induction in wild-type mice (Fig. 7A). Western blot analysis indicated that ERK phosphorylation was significantly reduced when slices were incubated with U0126 at concentrations of either 1 μM (approximately 30% inhibition) or 5μM (approximately 80% inhibition), but not at 100 nM (Fig. 7A). To determine whether

the elevated MEK-ERK signaling was involved in the impaired mGluR-LTD, hippocampal slices from ΔRG mice and their wild-type littermates were treated with DHPG in the presence of U0126 (1 μM). Treatment with U0126 rescued the mGluR-LTD deficit observed in hippocampal slices from ΔRG mice (Fig. 7B, right panel). The effect of U0126 was specific to mGluR-LTD in ΔRG mice, because this concentration of the drug did not significantly impact mGluR-LTD in wild-type littermates (Fig. 7B, left panel). To determine whether treatment of ΔRG hippocampal slices with U0126 rescued mGluR-LTD back to the same level of control groups (WT + vehicle; WT + U0126) we analyzed the average fEPSP slopes from WT and ΔRG hippocampal slices in the presence of the vehicle or U0126 during the time period of 20 to 50 min after the washout of DHPG. We found that treatment with U0126 returned mGluR-LTD in ΔRG mice back to levels observed in WT mice (Fig. 7C). We then determined whether treatment with DHPG resulted in a further increase in ERK phosphorylation in ΔRG mice. Hippocampal slices were treated with DHPG and area CA1 was isolated. Western blot data showed a significant increase of ERK phosphorylation in slices from ΔRG mice treated with DHPG (Fig. 8A). In addition, Western Blot analysis from area CA1 of hippocampal slices collected after the rescue experiment confirmed the reduction of ERK phosphorylation by U0126 (1μM) (Fig. 8B). Taken together, these findings are consistent with the idea that the impaired hippocampal mGluR-LTD exhibited by ΔRG mice is due to enhanced MEK-ERK signaling.

Discussion

Our examination of hippocampal synaptic plasticity in the ΔRG mouse model of TSC resulted in several unexpected findings. First, we observed that both E-LTP and L-LTP were unaltered in ΔRG mice (Fig. 3A and 3B). In contrast, E-LTP-inducing stimulation was shown to produce stable, rapamycin-sensitive, L-LTP in TSC2 heterozygous knockout mice (Ehninger et al., 2008). It appears that in the complete absence of one allele, as in the case of TSC2 heterozygous knockout mice, the impact on mTORC1 signaling is more robust and broader than in the case of having specific mutations in the TSC2-GAP domain as is present in the ΔRG mice. Indeed, we observed that mTORC1 signaling was not significantly altered in the ΔRG mice (Fig. 4), whereas mTORC1 signaling in both $TSC1^{+/-}$ cKO and $TSC2^{-/-}$ cKO mice were enhanced as shown by increase phosphorylation of S6K1 (Supplementary Fig. 1). The latter finding is consistent with recent studies where the hippocampal deletion of the *Tsc1* gene resulted in enhanced mTORC1 signaling (Bateup et al., 2011). The second unexpected finding was that mGluR-LTD was impaired in the ΔRG mice (Fig. 3D). Moreover, the ΔRG mice exhibited normal NMDAR-LTD in (Fig. 3C), similar to recent findings in mice with virally-mediated deletion of the *Tsc1* gene in the hippocampus (Bateup et al., 2011). Thus, disruption of TSC2-GAP function, either by GAP mutations or decreasing TSC1/2 heterodimer stability compromising TSC2-GAP activity, interferes with distinct molecular mechanisms required for the expression of mGluR-LTD but not NMDAR-LTD.

mGluR-LTD in both $TSC1^{+/-}$ cKO and $TSC2^{-/-}$ cKO mice was impaired at the same level as it was in ΔRG mice (Fig. 4C). Our findings with $TSC1^{+/-}$ cKO mice (Fig. 4A) confirm recent studies showing that the loss of *Tsc1* impairs hippocampal mGluR-LTD (Bateup et al., 2011). The impaired mGluR-LTD in ΔRG mice was unexpected because mGluR-LTD, ERK phosphorylation, and mTORC1 signaling are enhanced in FXS model mice that lack FMRP, a translation suppressor (Hou et al., 2006; Sharma et al., 2010). It is possible that there are different subcellular pools of ERK that are activated in ΔRG mice and FXS mice that results in the phosphorylation of dissimilar ERK substrates that impact mGluR-LTD differently. Interestingly, the mGluR-LTD phenotype in the ΔRG mouse model of TSC differs from FXS model mice lacking FMRP, but more closely approximates that observed in transgenic mice overexpressing FMRP, which exhibit completely abolished mGluR-LTD

(Hou et al., 2006). Thus, ΔRG mice and FXS mice are examples of two types of improper activation of ERK and mTORC1 signaling in the brain. In ΔRG mice, robust enhancement of ERK signaling results in impaired mGluR-LTD, whereas modest activation of ERK and mTORC1 signaling in FXS model mice results in enhanced mGluR-LTD (Hou et al., 2006; Sharma et al., 2010).

Although upregulated mTORC1 signaling has been reported in other mouse models of TSC and FXS (Bateup et al., 2011; Ehninger et al., 2008; Sharma et al., 2010), the mutation in the TSC2-GAP domain in the ΔRG mice appears to recruit an mTORC1-independent mechanism in the hippocampus, the third unexpected finding in our studies. Normally, TSC2 negatively regulates Rheb, which is immediately upstream of mTORC1 (Tee et al., 2003). Active, GTP-bound Rheb also has been shown to negatively regulate Ras/B-Raf/C-Raf/MEK signaling by disrupting B-Raf/C-Raf heterodimerization (Im et al., 2002; Karbowniczek et al., 2006). B-Raf has a high basal kinase activity toward MEK1/2, and is now available to participate in the activation Rap1/Epac/B-Raf signaling pathway (Moodie et al., 1994; Papin et al., 1998; Papin et al., 1996; Reuter et al., 1995; Wang et al., 2006), which is then a potential mechanism for the upregulated ERK phosphorylation and S6 235/236 phoshporylation observed in the ΔRG mice (Fig. 5A and 5C). In fact, the impaired mGluR-LTD observed in ΔRG mice was rescued with the MEK inhibitor U0126, supporting the idea that elevated MEK-ERK signaling contributes to synaptic abnormalities in these mice (Fig. 7B). Moreover, the enhanced basal phosphorylation of ERK in ΔRG mice is further increased by DHPG treatment (Fig. 8A). In contrast, conditional deletion of *Tsc1* and *Tsc2* genes in the forebrain did not result in upregulated ERK phosphorylation (Fig. 6) Thus, it is possible that synaptic and behavioral phenotypes in mice with conditional deletions of *Tsc1* and *Tsc2* might be due to exaggerated mTORC1 signaling (Supplementary Fig. 1B) (Bateup et al., 2011; Ehninger et al., 2008) in contrast to the ΔRG mice where the phenotypes are due to exaggerated ERK signaling.

An additional potential mechanism for the elevated ERK phosphorylation we observed in the ΔRG mice is altered activity of the striatal-enriched protein tyrosine phosphatase (STEP). STEP is a phosphatase shown to regulate synaptic function by modulating NMDA and AMPA receptor trafficking, as well as ERK phosphorylation and nuclear translocation (Braithwaite et al., 2006; Paul et al., 2003; Snyder et al., 2005). In addition, studies have shown that STEP translation is triggered by activation of group I mGluRs and subsequent activation of the ERK, PI3K and mTORC1 pathways (Zhang et al., 2008). It remains to be determined whether dysregulation of STEP is involved in the elevated ERK phosphorylation observed in the ΔRG mice.

Importantly, in accordance with our findings, analyses of brain lesions and tumors associated with TSC have shown aberrantly activated ERK that is correlated with increased phosphorylation of ribosomal protein S6 (Jozwiak et al., 2008; Ma et al., 2005; Ma et al., 2007). Thus, simultaneous treatment with inhibitors of both mTORC1 and ERK signaling pathways could be an effective treatment for TSC patients. Future studies will be required to delineate the molecular mechanism resulting in altered TSC1/2-ERK signaling and whether it is involved in any cognitive and behavioral abnormalities displayed by the ΔRG mice.

Conclusions

Our studies herein show that disruptive mutations of the GAP domain of TSC2 impairs the expression of mGluR-LTD in ΔRG mice, without affecting NMDAR-dependent LTD. Moreover, rescue experiments with the MEK inhibitor U0126 supports the idea that mutations in the TSC2-GAP domain in the ΔRG mice recruits an ERK-dependent and mTORC1-independent mechanism, resulting in impaired mGluR-LTD. In contrast, MEK-ERK signaling appears to be normal but mTORC1 signaling is elevated in mice with

conditional deletion of *Tsc1* and *Tsc2* genes, suggesting that impaired mGluR-LTD in these mice is due to exaggerated mTORC1 signaling. Consequently, ΔRG mice is a mouse model of TSC that can be used to study the role of both TSC2-GAP domain and TSC1/2-ERK signaling in abnormal synaptic plasticity associated with TSC.

Research Highlights

- Mutations in TSC2-GAP domain disrupt hippocampal mGluR-LTD in ΔRG mice.
- ΔRG mice exhibit normal mTORC1 signaling, but enhanced ERK signaling.
- Impaired hippocampal mGluR-LTD is due to aberrant MEK/ERK singnaling in ΔRG mice.
- Mice with conditional deletions of the *Tsc1* and *Tsc2* genes exhibit deficits in mGluR-LTD, but normal MEK/ERK signaling

Supplementary Material

Refer to Web version on PubMed Central for supplementary material.

Abbreviations

4E-BP	eIF4E binding protein
ACSF	artificial cerebrospinal fluid
CMV	cytomegalovirus
FXS	fragile X syndrome
GAP	GTPase-activating protein
GDP	guanosine diphosphate
GTP	guanosine triphosphate
mTORC1	mammalian trget of rapamycin complex 1
Rheb	Ras homologenrinched in brain
STEP	striatal-enrinched tyrosine phosphatase
TSC	tuberous sclerosis complex

Acknowledgments

This work was supported by National Institutes of Health grants NS034007 and NS047384 (E.K.), and MH085489 (I.C.T.).

References

Banko JL, et al. Regulation of eukaryotic initiation factor 4E by converging signaling pathways during metabotropic glutamate receptor-dependent long-term depression. J Neurosci. 2006; 26:2167–2173. [PubMed: 16495443]

Bateup HS, et al. Loss of Tsc1 In Vivo Impairs Hippocampal mGluR-LTD and Increases Excitatory Synaptic Function. J Neurosci. 2011; 31:8862–8869. [PubMed: 21677170]

Bhatia B, et al. Tuberous sclerosis complex suppression in cerebellar development and medulloblastoma: separate regulation of mammalian target of rapamycin activity and p27 Kip1 localization. Cancer Res. 2009; 69:7224–7234. [PubMed: 19738049]

Boer K, et al. Cellular localization of metabotropic glutamate receptors in cortical tubers and subependymal giant cell tumorFs of tuberous sclerosis complex. Neuroscience. 2008; 156:203–215. [PubMed: 18706978]

Braithwaite SP, et al. Synaptic plasticity: one STEP at a time. Trends Neurosci. 2006; 29:452–458. [PubMed: 16806510]

Cai SL, et al. Activity of TSC2 is inhibited by AKT-mediated phosphorylation and membrane partitioning. J Cell Biol. 2006; 173:279–289. [PubMed: 16636147]

Camposano SE, et al. Distinct clinical characteristics of tuberous sclerosis complex patients with no mutation identified. Ann Hum Genet. 2009; 73:141–146. [PubMed: 19133941]

Cheadle JP, et al. Molecular genetic advances in tuberous sclerosis. Hum Genet. 2000; 107:97–114. [PubMed: 11030407]

Chévere-Torres I, et al. Impaired social interactions and motor learning in tuberous sclerosis complex model mice expressing a dominant/negative form of tuberin. Neurobiol. Dis. 2012 in press.

Dabora SL, et al. Mutational analysis in a cohort of 224 tuberous sclerosis patients indicates increased severity of TSC2, compared with TSC1, disease in multiple organs. Am J Hum Genet. 2001; 68:64–80. [PubMed: 11112665]

DiMario FJ Jr. Brain abnormalities in tuberous sclerosis complex. J Child Neurol. 2004; 19:650–657. [PubMed: 15563010]

Ehninger D, et al. Reversal of learning deficits in a Tsc2+/− mouse model of tuberous sclerosis. Nat Med. 2008; 14:843–848. [PubMed: 18568033]

Ehninger D, Silva AJ. Increased Levels of Anxiety-related Behaviors in a Tsc2 Dominant Negative Transgenic Mouse Model of Tuberous Sclerosis. Behav Genet. 2010

Favata MF, et al. Identification of a novel inhibitor of mitogen-activated protein kinase kinase. J Biol Chem. 1998; 273:18623–18632. [PubMed: 9660836]

Gallagher SM, et al. Extracellular signal-regulated protein kinase activation is required for metabotropic glutamate receptor-dependent long-term depression in hippocampal area CA1. J Neurosci. 2004; 24:4859–4864. [PubMed: 15152046]

Govindarajan B, et al. Transgenic expression of dominant negative tuberin through a strong constitutive promoter results in a tissue-specific tuberous sclerosis phenotype in the skin and brain. J Biol Chem. 2005; 280:5870–5874. [PubMed: 15576369]

Hernandez O, et al. Generation of a conditional disruption of the Tsc2 gene. Genesis. 2007; 45:101–106. [PubMed: 17245776]

Hou L, et al. Dynamic translational and proteasomal regulation of fragile X mental retardation protein controls mGluR-dependent long-term depression. Neuron. 2006; 51:441–454. [PubMed: 16908410]

Hou L, Klann E. Activation of the phosphoinositide 3-kinase-Akt-mammalian target of rapamycin signaling pathway is required for metabotropic glutamate receptor-dependent long-term depression. J Neurosci. 2004; 24:6352–6361. [PubMed: 15254091]

Huber KM, et al. Altered synaptic plasticity in a mouse model of fragile X mental retardation. Proc Natl Acad Sci U S A. 2002; 99:7746–7750. [PubMed: 12032354]

Im E, et al. Rheb is in a high activation state and inhibits B-Raf kinase in mammalian cells. Oncogene. 2002; 21:6356–6365. [PubMed: 12214276]

Jansen AC, et al. Unusually mild tuberous sclerosis phenotype is associated with TSC2 R905Q mutation. Ann Neurol. 2006; 60:528–539. [PubMed: 17120248]

Jones AC, et al. Molecular genetic and phenotypic analysis reveals differences between TSC1 and TSC2 associated familial and sporadic tuberous sclerosis. Hum Mol Genet. 1997; 6:2155–2161. [PubMed: 9328481]

Jozwiak J. Hamartin and tuberin: working together for tumour suppression. Int J Cancer. 2006; 118:1–5. [PubMed: 16206276]

Jozwiak J, et al. Positive and negative regulation of TSC2 activity and its effects on downstream effectors of the mTOR pathway. Neuromolecular Med. 2005; 7:287–296. [PubMed: 16391386]

Jozwiak J, et al. Possible mechanisms of disease development in tuberous sclerosis. Lancet Oncol. 2008; 9:73–79. [PubMed: 18177819]

Karbowniczek M, et al. Rheb inhibits C-raf activity and B-raf/C-raf heterodimerization. J Biol Chem. 2006; 281:25447–25456. [PubMed: 16803888]

Krymskaya VP. Tumour suppressors hamartin and tuberin: intracellular signalling. Cell Signal. 2003; 15:729–739. [PubMed: 12781866]

Kwiatkowski DJ. Tuberous sclerosis: from tubers to mTOR. Ann Hum Genet. 2003; 67:87–96. [PubMed: 12556239]

Kwiatkowski DJ, et al. A mouse model of TSC1 reveals sex-dependent lethality from liver hemangiomas, and up-regulation of p70S6 kinase activity in Tsc1 null cells. Hum Mol Genet. 2002; 11:525–534. [PubMed: 11875047]

Ma L, et al. Phosphorylation and functional inactivation of TSC2 by Erk implications for tuberous sclerosis and cancer pathogenesis. Cell. 2005; 121:179–193. [PubMed: 15851026]

Ma L, et al. Identification of S664 TSC2 phosphorylation as a marker for extracellular signal-regulated kinase mediated mTOR activation in tuberous sclerosis and human cancer. Cancer Res. 2007; 67:7106–7112. [PubMed: 17671177]

Maheshwar MM, et al. The GAP-related domain of tuberin, the product of the TSC2 gene, is a target for missense mutations in tuberous sclerosis. Hum Mol Genet. 1997; 6:1991–1996. [PubMed: 9302281]

Moodie SA, et al. Association of MEK1 with p21ras.GMPPNP is dependent on B-Raf. Mol Cell Biol. 1994; 14:7153–7162. [PubMed: 7935430]

Orlova KA, Crino PB. The tuberous sclerosis complex. Ann N Y Acad Sci. 2010; 1184:87–105. [PubMed: 20146692]

Osterweil EK, et al. Hypersensitivity to mGluR5 and ERK1/2 leads to excessive protein synthesis in the hippocampus of a mouse model of fragile X syndrome. J Neurosci. 2010; 30:15616–15627. [PubMed: 21084617]

Papin C, et al. Modulation of kinase activity and oncogenic properties by alternative splicing reveals a novel regulatory mechanism for B-Raf. J Biol Chem. 1998; 273:24939–24947. [PubMed: 9733801]

Papin C, et al. Identification of signalling proteins interacting with B-Raf in the yeast two-hybrid system. Oncogene. 1996; 12:2213–2221. [PubMed: 8668348]

Pasumarthi KB, et al. Enhanced cardiomyocyte DNA synthesis during myocardial hypertrophy in mice expressing a modified TSC2 transgene. Circ Res. 2000; 86:1069–1077. [PubMed: 10827137]

Paul S, et al. NMDA-mediated activation of the tyrosine phosphatase STEP regulates the duration of ERK signaling. Nat Neurosci. 2003; 6:34–42. [PubMed: 12483215]

Pende M, et al. S6K1(−/−)/S6K2(−/−) mice exhibit perinatal lethality and rapamycin-sensitive 5'-terminal oligopyrimidine mRNA translation and reveal a mitogen-activated protein kinase-dependent S6 kinase pathway. Mol Cell Biol. 2004; 24:3112–3124. [PubMed: 15060135]

Reuter CW, et al. Biochemical analysis of MEK activation in NIH3T3 fibroblasts. Identification of B-Raf and other activators. J Biol Chem. 1995; 270:7644–7655. [PubMed: 7706312]

Richter JD, Klann E. Making synaptic plasticity and memory last: mechanisms of translational regulation. Genes Dev. 2009; 23:1–11. [PubMed: 19136621]

Ronesi JA, Huber KM. Metabotropic glutamate receptors and fragile x mental retardation protein: partners in translational regulation at the synapse. Sci Signal. 2008; 1:pe6. [PubMed: 18272470]

Roux PP, et al. Tumor-promoting phorbol esters and activated Ras inactivate the tuberous sclerosis tumor suppressor complex via p90 ribosomal S6 kinase. Proc Natl Acad Sci U S A. 2004; 101:13489–13494. [PubMed: 15342917]

Sambucetti LC, et al. NF-kappa B activation of the cytomegalovirus enhancer is mediated by a viral transactivator and by T cell stimulation. EMBO J. 1989; 8:4251–4258. [PubMed: 2556267]

Sharma A, et al. Dysregulation of mTOR signaling in fragile X syndrome. J Neurosci. 2010; 30:694–702. [PubMed: 20071534]

Snyder EM, et al. Regulation of NMDA receptor trafficking by amyloid-beta. Nat Neurosci. 2005; 8:1051–1058. [PubMed: 16025111]

Tavazoie SF, et al. Regulation of neuronal morphology and function by the tumor suppressors Tsc1 and Tsc2. Nat Neurosci. 2005; 8:1727–1734. [PubMed: 16286931]

Tee AR, et al. Tuberous sclerosis complex gene products, Tuberin and Hamartin, control mTOR signaling by acting as a GTPase-activating protein complex toward Rheb. Curr Biol. 2003; 13:1259–1268. [PubMed: 12906785]

Uhlmann EJ, et al. Loss of tuberous sclerosis complex 1 (Tsc1) expression results in increased Rheb/S6K pathway signaling important for astrocyte cell size regulation. Glia. 2004; 47:180–188. [PubMed: 15185396]

Wang Y, et al. Neocortical hyperexcitability in a human case of tuberous sclerosis complex and mice lacking neuronal expression of TSC1. Ann Neurol. 2007; 61:139–152. [PubMed: 17279540]

Wang Z, et al. Rap1-mediated activation of extracellular signal-regulated kinases by cyclic AMP is dependent on the mode of Rap1 activation. Mol Cell Biol. 2006; 26:2130–2145. [PubMed: 16507992]

Yang Q, et al. TSC1/TSC2 and Rheb have different effects on TORC1 and TORC2 activity. Proc Natl Acad Sci U S A. 2006; 103:6811–6816. [PubMed: 16627617]

Zhang Y, et al. Rheb is a direct target of the tuberous sclerosis tumour suppressor proteins. Nat Cell Biol. 2003; 5:578–581. [PubMed: 12771962]

Zhang Y, et al. The tyrosine phosphatase STEP mediates AMPA receptor endocytosis after metabotropic glutamate receptor stimulation. J Neurosci. 2008; 28:10561–10566. [PubMed: 18923032]

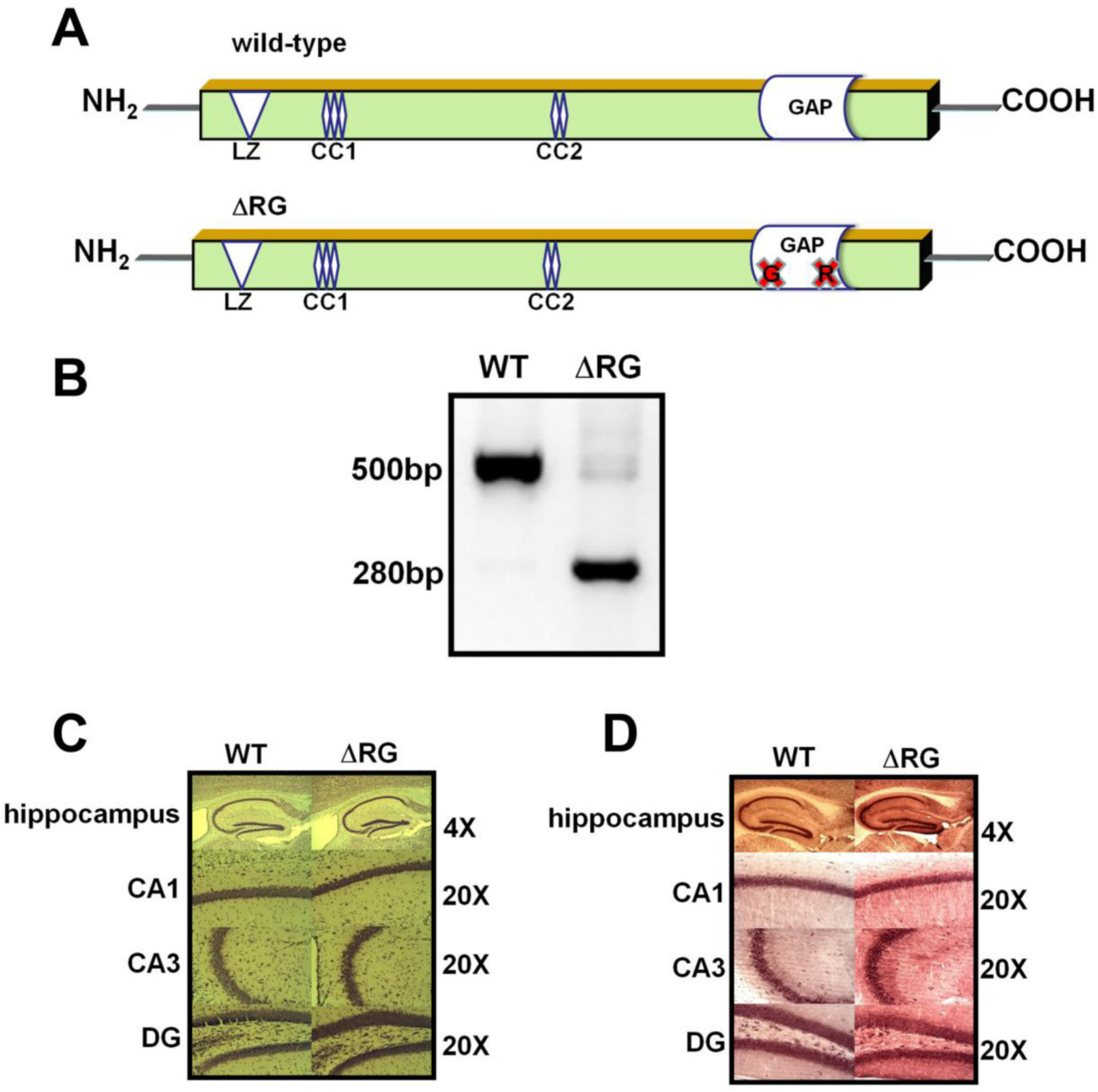

Figure 1.

Overexpression of ΔRG TSC2 protein in mouse hippocampus. (A) Schematic representation of the dominant negative TSC2 ΔRG in mice that model tuberous sclerosis. (B) PCR identification of ΔRG transgene showed a corresponding band at 280bp. The wild-type band is detected at 500bp. (C) Hippocampal morphology in ΔRG mice. Nissl staining of saggital sections showed no obvious aberrant morphology. (D) Immunolocalization of TSC2 in the mouse hippocampus. Increased levels of TSC2 were observed in hippocampal areas CA1 and CA3, and the dentate gyrus (DG) of ΔRG mice compared to WT mice.

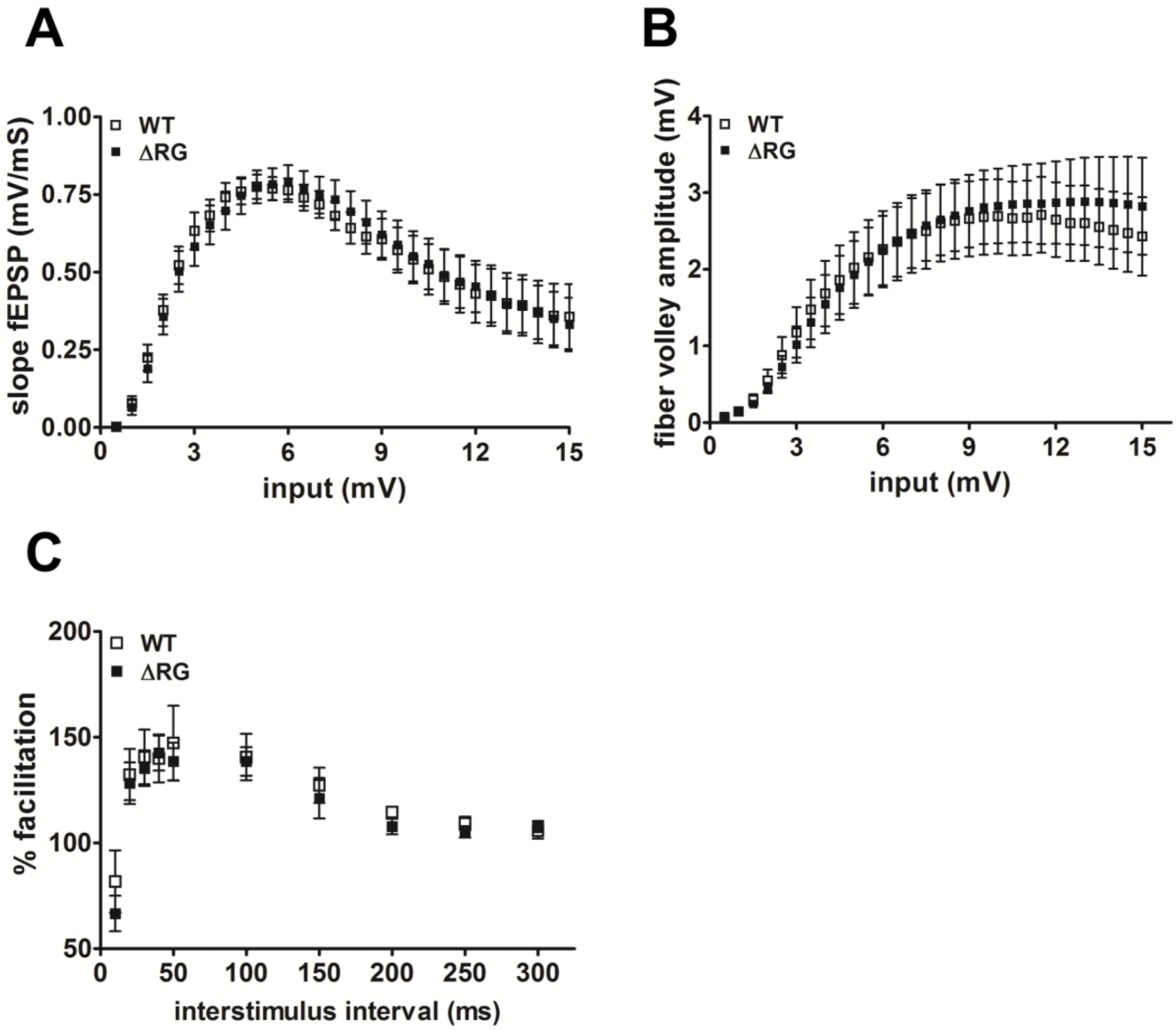

Figure 2.

ΔRG mice have normal basal synaptic transmission and paired-pulse facilitation. (A) Input/output plot indicates that both wild-type (WT) and ΔRG mice had comparable fEPSP slopes with increasing stimulation intensities, indicating normal postsynaptic function (WT, n=16; ΔRG, n=13; 2–3 slices/mouse per genotype. $P<0.05$, ANOVA). (B) Input/output plot indicates that both wild-type (WT) and ΔRG mice had comparable fiber volley amplitude with increasing stimulation intensities, indicating normal presynaptic function (WT, n=14; ΔRG, n=17; 2–3 slices/mouse per genotype. $P<0.05$, ANOVA). (C) ΔRG mice exhibit normal paired-pulse facilitation (PPF) compared to their WT littermates using interpulse intervals ranging from 10 to 300 ms. The percent of facilitation was calculated from the ratio of the second fEPSP to the first fEPSP (WT, n=8; ΔRG, n=8; 2–3 slices/mouse per genotype. $P<0.05$, ANOVA).

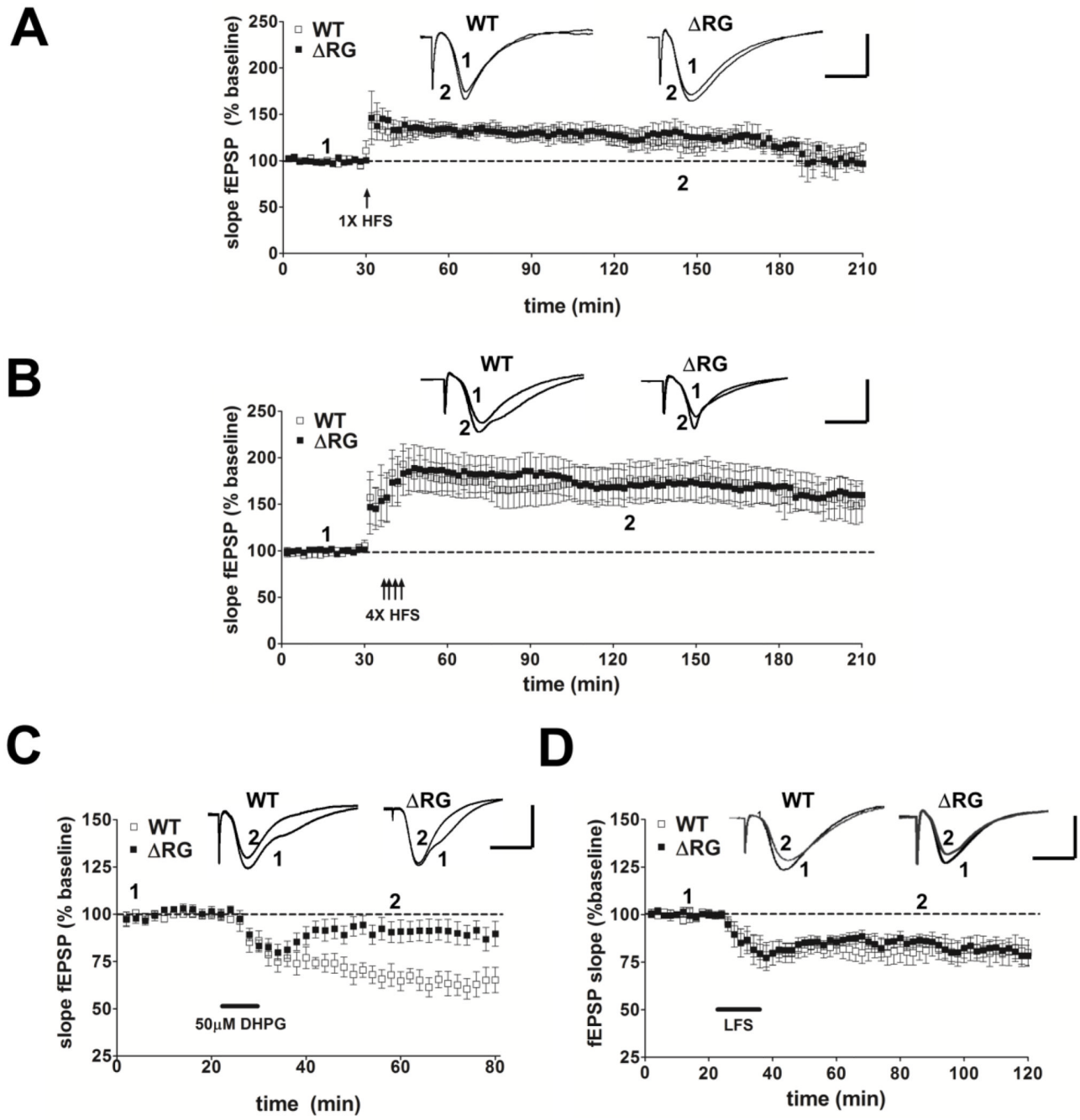

Figure 3.

ΔRG mice have normal hippocampal E-LTP, L-LTP and NMDAR-LTD but have impaired mGluR-LTD. (A) Top, representative fEPSPs in slices from wild-type (WT) and ΔRG mice before and after receiving one train of HFS. Calibration: 5 mV, 5 ms. Bottom, a single train of HFS elicits similar levels of E-LTP in WT and ΔRG mice (WT, n= 7; ΔRG, n=7; 2–3 slices/mouse per genotype. P>0.05, ANOVA). (B). Top, representative fEPSPs in slices from WT and ΔRG mice before and after receiving four trains of HFS. Bottom, four trains of HFS elicited similar levels of L-LTP in WT and ΔRG mice (WT, n=10; ΔRG, n=15; 2–3 slices/mouse per genotype. P>0.05, ANOVA). (C) Top, representative fEPSPs in slices from WT and ΔRG mice before and after treatment with DHPG (50 μM, 10 min) to induce

mGLUR-LTD. Bottom, DHPG application induced LTD in WT mice, but not in ΔRG mice (WT, n=7; ΔRG, n=8; 2–3 slices/mouse per genotype. **p<0.01, ANOVA). (D) Top, representative fEPSPs in slices from wild-type (WT) and ΔRG mice before and after receiving 900 pulses of LFS for 15 min. Bottom, LFS elicits similar levels of NMDR-LTD in WT and ΔRG mice (WT, n= 12; ΔRG, n=12; 3 slices/mouse per genotype. P>0.05, ANOVA).

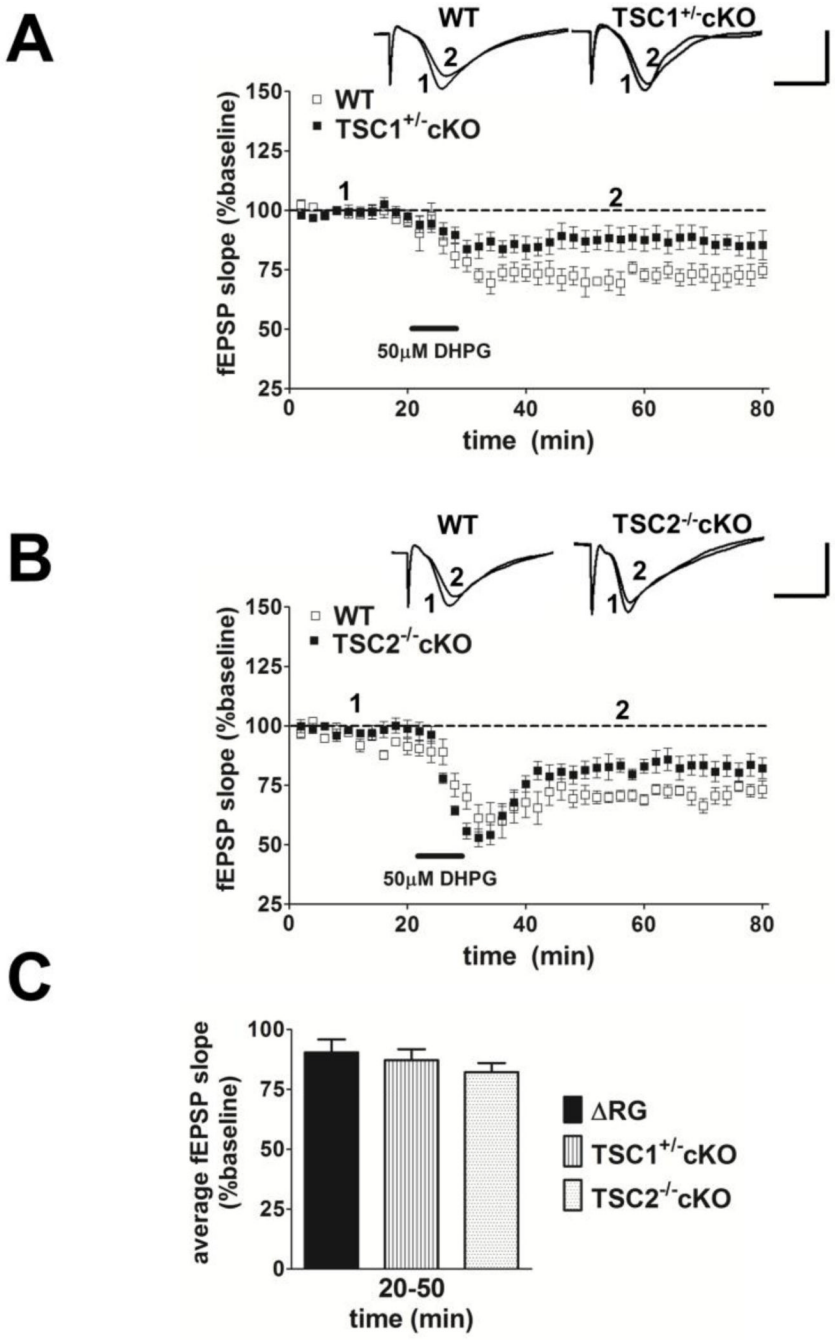

Figure 4.

mGluR-LTD is impaired in mice with conditional deletions of TSC1 and TSC2. (A) Top, representative fEPSPs in slices from WT and $TSC1^{+/-}$ cKO mice before and after treatment with DHPG (50 μM, 10 min) to induce mGLUR-LTD. Calibration: 5 mV, 5 ms. Bottom, DHPG application induced LTD in WT mice and impaired LTD in $TSC1^{+/-}$ cKO (WT, n=4; $TSC1^{+/-}$ cKO, n=8; 2–3 slices/mouse per genotype. *p<0.05, ANOVA). (B) Top, representative fEPSPs in slices from WT and $TSC2^{-/-}$ cKO mice before and after treatment with DHPG (50μM, 10 min) to induce mGLUR-LTD. Bottom, DHPG application induced LTD in WT mice and impaired LTD in $TSC2^{-/-}$ cKO (WT, n=8; $TSC2^{-/-}$ cKO, n=4; 1–2 slices/mouse per genotype. *p<0.05, ANOVA). (C) Bar graph depicting average fEPSP

slope 20 to 50 min after the washout of DHPG. DHPG application induced same level of mGluR-LTD in ΔRG, $TSC1^{+/-}$ cKO, and $TSC2^{-/-}$ cKO mice (ΔRG, n=8; $TSC1^{+/-}$ cKO, n=8; $TSC2^{-/-}$ cKO, n=4. $p>0.05$, Student's *t*-test compared with ΔRG for the given time period).

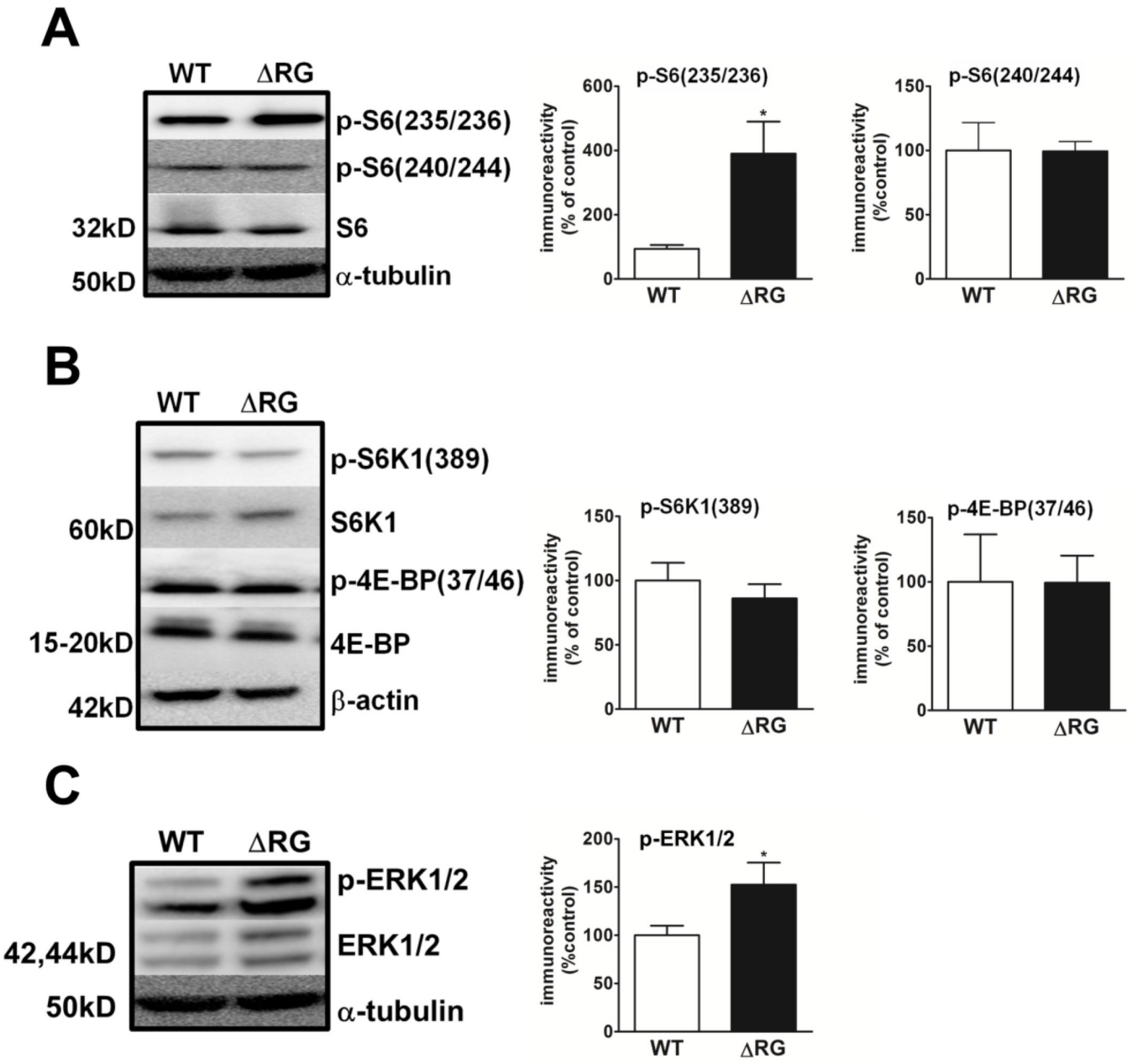

Figure 5.

mTORC1 signaling is unaltered, but S6 and ERK phosphorylation are elevated in the hippocampus of ΔRG mice. (A) S6 phosphorylation at serine 235/236 is increased, whereas phosphorylation at serine 240/244 is not altered in the hippocampus of ΔRG mice (WT, n=3; ΔRG n=4. *p<0.05, Student's *t*-test). (B) Phosphorylation of 4E-BP (WT, n=3; ΔRG n=3). P>0.05, Student's *t*-test) and S6K1 are unaltered (WT, n=4; ΔRG n=6). P>0.05, Student's *t*-test) in ΔRG mice. (C) ERK1/2 phosphorylation is increased in ΔRG mice (WT, n=3; ΔRG n=3). *p<0.05, Student's *t*-test). Phospho-protein phosphorylation immunoreactivity was normalized to tubulin and its corresponding total protein immunoreactivity.

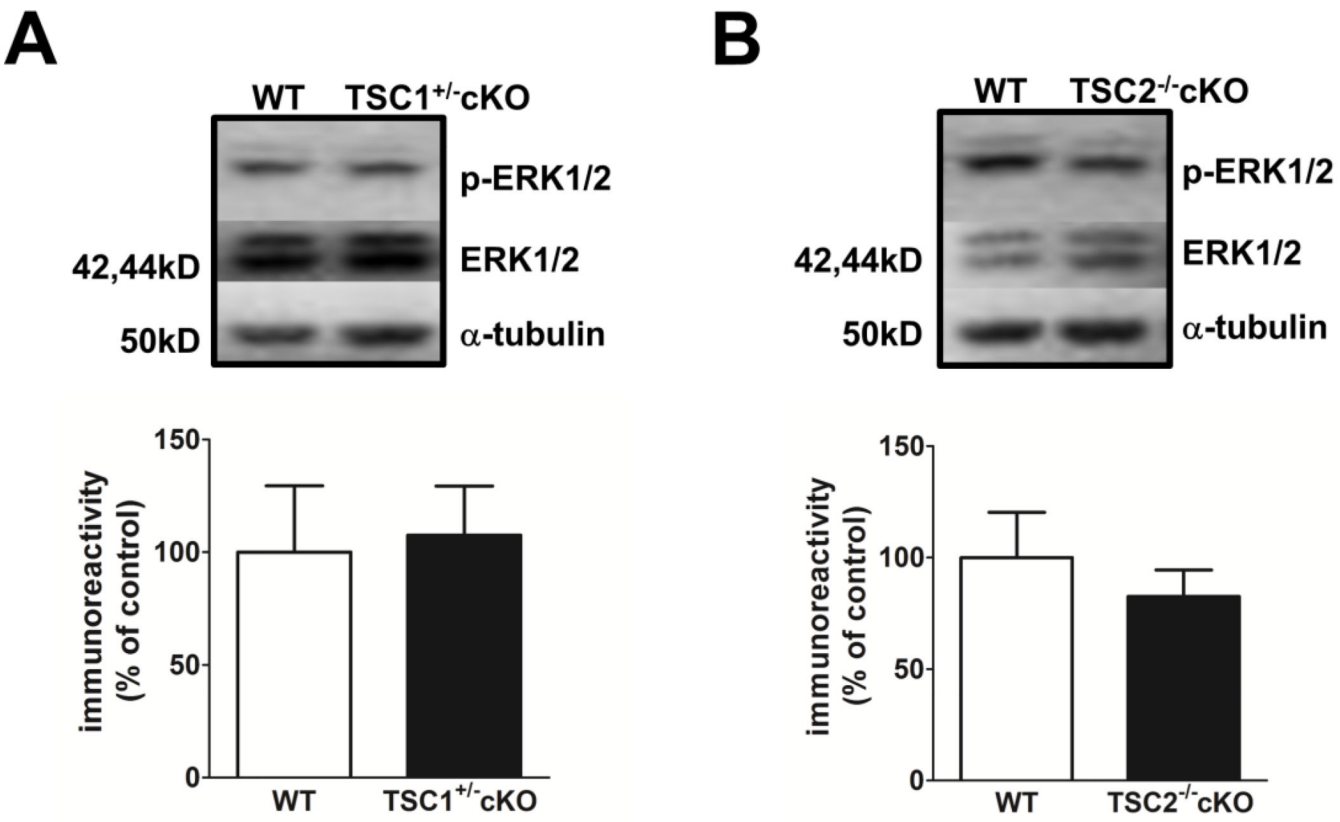

Figure 6.

ERK signaling is unaltered in the hippocampus of $TSC1^{+/-}$ cKO and $TSC2^{-/-}$ cKO mice. (A) Basal ERK1/2 phosphorylation is normal in $TSC1^{+/-}$ cKO mice (WT, n=3; $TSC1^{+/-}$ cKO, n=3). P>0.05, Student's *t*-test). (B) Basal ERK1/2 phosphorylation is normal in $TSC2^{-/-}$ cKO mice (WT, n=3; $TSC2^{-/-}$ cKO, n=3). P>0.05, Student's *t*-test). ERK1/2 phosphorylation immunoreactivity was normalized to tubulin and total ERK1/2 immunoreactivity.

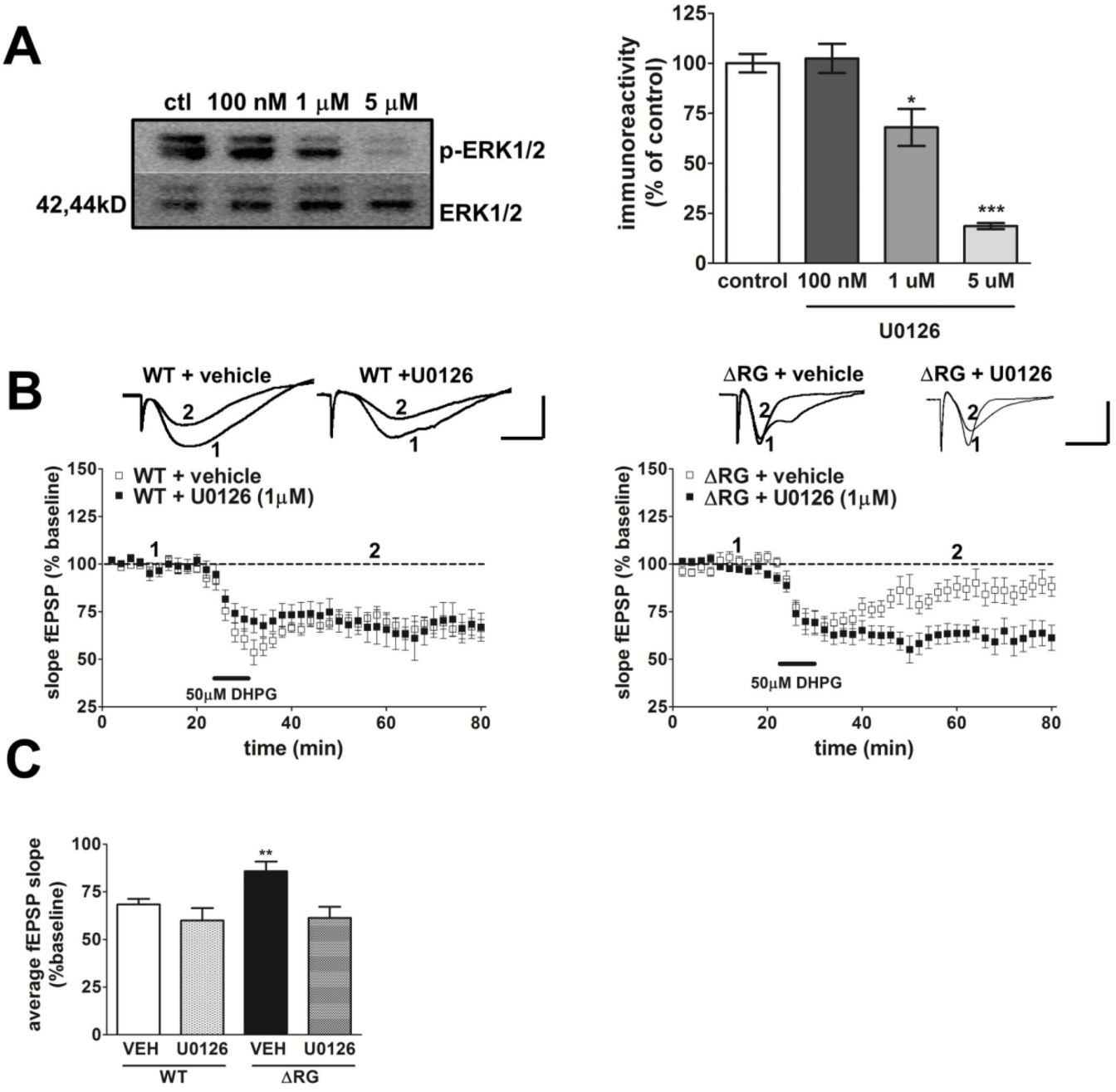

Figure 7.

Impaired mGluR-LTD in ΔRG mice is rescued by inhibition of MEK-ERK signaling. (A) Incubation of wild-type (WT) hippocampal slices for 30 min with 100 nM U0126 did not alter, whereas incubation with 1 μM and 5 μM U0126 significantly decreased ERK phosphorylation (n=6 mice; 2–3 slices per treatment. ***p<0.0001, one-way ANOVA analysis followed by Dunnett's test [control vs. 100 nM, p>0.05; control vs. 1 μM, **p<0.001; control vs. 5 μM, ***p<0.0001]). (B) Left panel: Top, representative fEPSPs in slices from WT mice before and after treatment with DHPG (50 μM, 10 min) to induce mGluR-LTD in the presence of either vehicle (DMSO) or U0126 (1μM). Calibration: 5 mV, 5 ms. Bottom, mGluR-LTD was induced by DHPG application in the presence of either

vehicle or 1 μM U0126 in WT mice (WT + vehicle, n=14; WT + U0126, n=14; 1–2 slices/mouse per drug treatment. P>0.05, ANOVA). Right panel: top, representative fEPSPs in slices from ΔRG mice before and after treatment with DHPG (50 μM, 10 min) to induce mGluR-LTD in the presence of either vehicle or U0126 (1μM). Bottom, mGluR-LTD was induced by DHPG application in the presence of 1 μM U0126, but not vehicle, in ΔRG mice (ΔRG + vehicle, n=12; ΔRG + U0126, n=13; 1–2 slices/mouse per drug treatment. ***p<0.0001, ANOVA). The vehicle and U0126 was present before, during and after DHPG application. (C) Left panel: bar graph depicting average fEPSP slope 20 to 50 min after the washout of DHPG in the presence of either vehicle or U0126 (WT + vehicle, n=14; WT + U0126, n=14; ΔRG + vehicle, n=12; ΔRG + U0126, n=13; **p<0.01, one-way ANOVA; [**p<0.05, Student's *t*-test compared with ΔRG + vehicle for the given time period]).

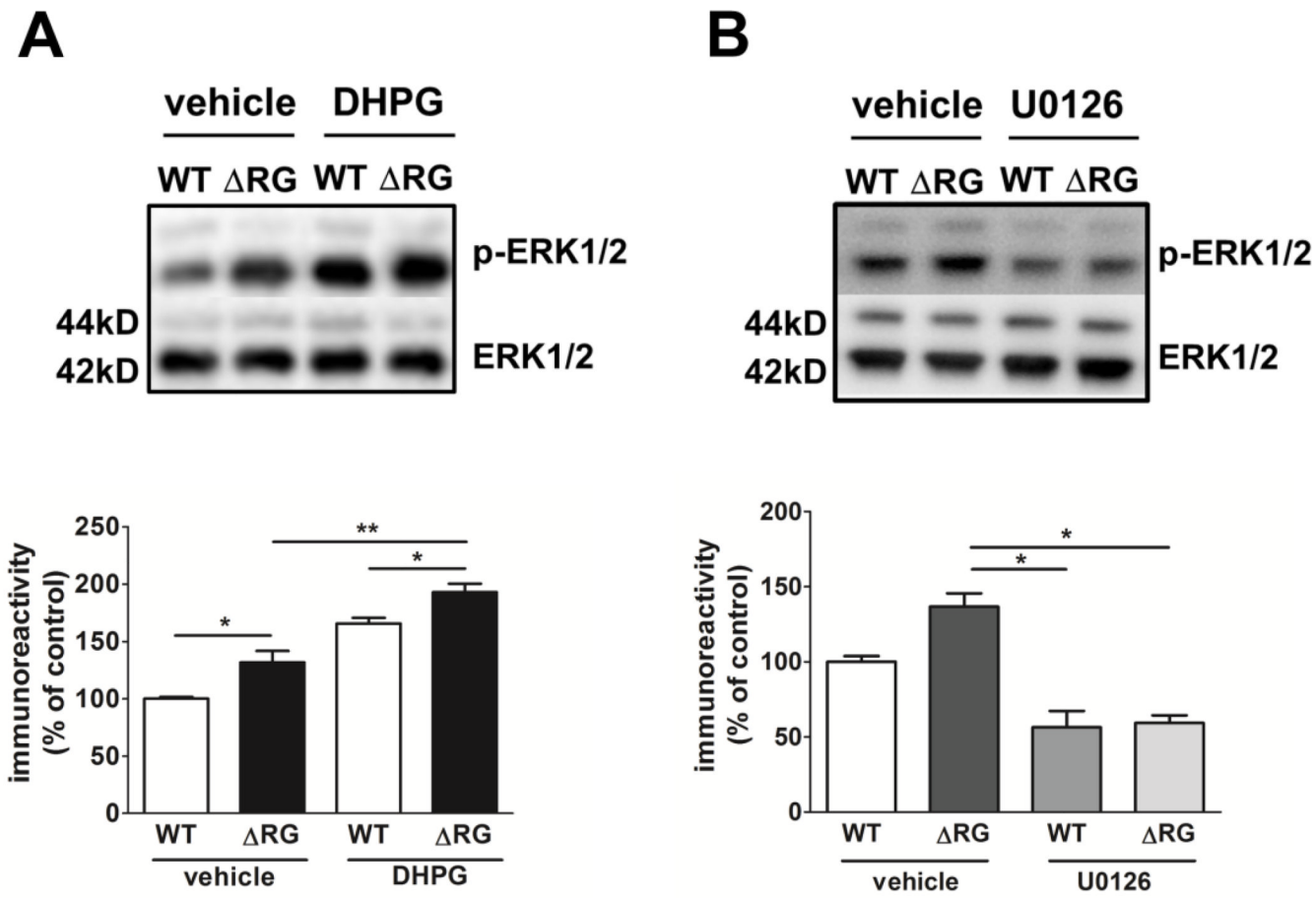

Figure 8.

Biochemical analysis of MEK/ERK signaling inhibition during mGluR-LTD induction in ΔRG mice. (A) ERK phosphorylation is further increased in area CA1 of hippocampal slices from ΔRG mice after treatment with DHPG (50 μM, 10 min) compared to hippocampal slices from wild-type (WT) mice treated with DHPG (n=3–4 slices per treatment. ***p<0.0001, one-way ANOVA analysis. Student's *t*-test [WT+ vehicle vs. ΔRG + vehicle, *p<0.05; WT+ DHPG vs. ΔRG + DHPG, *p<0.05; ΔRG + vehicle vs. ΔRG + DHPG, **p<0.01; WT + vehicle vs. WT + DHPG, ***p<0.0001]. (B) ERK phosphorylation is decreased in area CA1 from both WT and ΔRG hippocampal slices treated with U0126 (1 μM) after mGluR-LTD compared to control DMSO (n=6–8 slices per treatment. **p<0.01, one-way ANOVA analysis followed by Bonferroni's test [ΔRG + vehicle vs. WT + U0126, *p<0.05; ΔRG + vehicle vs. ΔRG + U0126, *p<0.05]).